LBL-11230
Preprint

Lawrence Berkeley Laboratory
UNIVERSITY OF CALIFORNIA

CHEMICAL BIODYNAMICS DIVISION

Submitted to The Journal of Chemical Physics

PHOTOVOLTAIC PROPERTIES OF AU-MEROCYANINE-TiO_2 SANDWICH CELLS
I. DARK ELECTRICAL PROPERTIES AND TRANSIENT EFFECTS

T. Skotheim, J.-M. Yang, J. Otvos, and M.P. Klein

July 1980

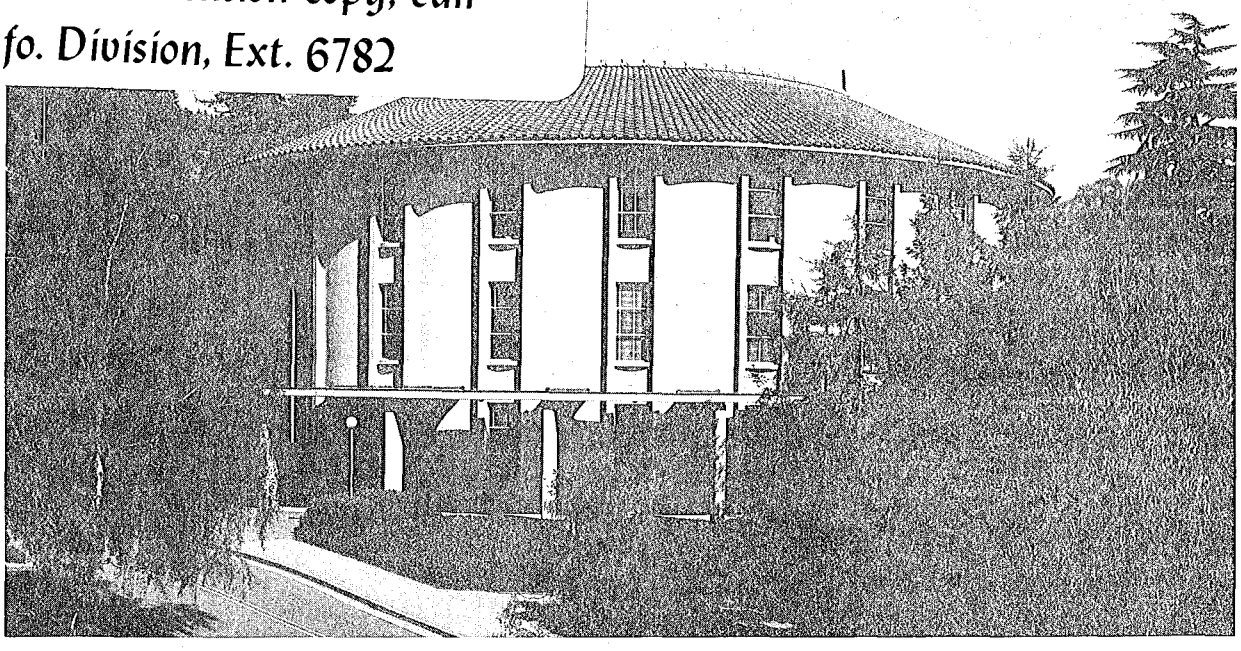

Prepared for the U.S. Department of Energy under Contract W-7405-ENG-48

Photovoltaic Properties of Au-Merocyanine-TiO_2 Sandwich Cells

I. Dark Electrical Properties and Transient Effects

T. Skotheim, J.-M. Yang, J. Otvos, and M.P. Klein

Laboratory of Chemical Biodynamics

Lawrence Berkeley Laboratory

University of California

Berkeley, California 94720

Abstract

The electrical properties of thin films (200-3000Å) of a merocyanine photosensitizing dye sandwiched between a TiO_2 single crystal doped n-type and a thin (200Å) Au metal layer has been studied. Dark current voltage measurements revealed that the current is space-charge limited at high current densities with an electron trapping density of approximately 10^{17} cm^{-3}. This was determined by using TiO_2 as an electron injecting contact. Interpretation of the kinetics of rise and decay of the photocurrent suggests that the mobility of holes, the majority carriers in merocyanine, is dependent on traps, the dominant trapping level having a depth of 0.11 eV. The decay of the photocurrent is monomolecular at short times and dominated by bimolecular recombination kinetics for long times of the order of seconds.

The high series resistance in the merocyanine prevents any band bending in the TiO_2, as the entire built-in voltage in the junction falls across the merocyanine film. This is supported by capacitance voltage data showing a complete absence of mobile charge carriers in the junction region.

I. Introduction

In this article and its companion, we report on our studies of various factors controlling the output efficiency in the photovoltaic mode of thin films of a merocyanine dye sandwiched between TiO_2 and Au.

The electrical properties in the dark and the kinetic effects associated with the photoconductive response are discussed in this paper. The following paper deals with the photovoltaic effects as well as the possibilities of doping the merocyanine film with electron acceptors and the effects of multilayers.

There have been a number of reports in the literature of studies of organic photoconductive compounds in the photovoltaic mode where a thin (0.1-1.0 μm) p-type organic photoconductor is interposed between two metals of different work functions (1-11). The high work function metal forms an ohmic or injecting electrode, and the low work function metal forms a barrier contact. Kearns and Calvin reported a photo-voltage of 200 mV for a sandwich structure of Mg-phthalocyanine coated with N,N,N',N'-tetramethyl-p-phenylenediamine with conductive glass as electrodes (12). Fedorov and Benderskii investigated Mg-phthalocyanine films sandwiched between Al and Ag contacts (5). They proposed a p-n junction model, formed by the replacement of Mg with Al in the dye-metal complex during heat treatment. They also reported dramatic changes in the photoconductive and photovoltaic properties when the films were doped with oxygen, with efficiency increases of one to three orders of magnitude for doped cells relative to the undoped ones. Ghosh et al. later reported studies of similar devices (4). Their results indicated the formation of a Schottky barrier at the low work function metal. The same mechanism has been supported by the results of Tang and

Albrecht (2), Merritt and Hovel (6), Kampas and Gouterman (8), and Fan and Faulkner (9) working on sandwich devices incorporating chlorophyll-a, 8-hydroxysquarylium, porphyrin derivatives, and phthalocyanines, respectively. Morel et al. (10) and Ghosh and Feng (11) in sandwiching merocyanine films between Al and Ag electrodes found higher efficiencies for cells which were exposed to air to enable an oxide layer to form prior to the deposition of the dye film. Their cells therefore had many of the characteristics of metal-oxide-semiconductor cells.

We have chosen a somewhat different approach in employing organic compounds in photovoltaic cells. It lies more in the tradition of photosensitization and the device could perhaps be called a dye-sensitized photovoltaic cell. Dye sensitization of semiconductors is well known from the photographic science literature (13-17). In recent years, a considerable amount of work has been done on photosensitization of wide band gap semiconductors by organic dyes adsorbed to the surface of the semiconductor (18,19).

The basic process of photosensitization of concern in the present work consists in the generation of a photocurrent on absorption of photons of energy less than the band gap of the semiconductor by monolayers or multilayers of dyes adsorbed onto the surface. A dye molecule adsorbed onto the surface of a semiconductor such that its highest occupied molecular orbital lies somewhere in the band gap and the lowest unoccupied molecular orbital somewhere above the bottom edge of the conduction band has the ability to photosensitize the semiconductor. This occurs via tunneling of an electron from the photoexcited dye molecule into the conduction band of the semiconductor where it can be drawn away by an appropriate electric field. In this manner, one may be able to extend the photosensitivity of the

semiconductor to longer wavelengths.

The present report is concerned with detailed studies of the trapping of mobile charges in the bulk of the merocyanine film and at the interfaces by means of measurements on forward current-voltage characteristics, transient effects, and by the kinetics of the photoconduction response. In addition, the C-V characteristics were also studied.

II. Experimental

The merocyanine dye used in these experiments (Fig. 1) was purchased from Gallard-Schlesinger Company and was used as purchased. The TiO_2 rutile single crystals were purchased from Nakazumi Crystals of Osaka, Japan. They were made semi-conductive by heating in a vacuum oven for two hours at 650°C and 5×10^{-6} torr. This treatment creates oxygen vacancies which act as donors (20). The crystals were slightly grey in color and were found to have a conductivity of 0.8 $ohm^{-1}cm^{-1}$.

The sandwich cell used in these experiments is diagrammed in Fig. 2. The TiO_2 crystals were polished with 1 micron alumina and etched fifteen minutes in sulfuric acid. The merocyanine and gold layers were sequentially deposited on the (001) face of the TiO_2 substrate by resistance heated thermal evaporation at a pressure of about 10^{-5} torr in a vacuum bell jar. The merocyanine was sublimed from a molybdenum basket heated by a tungsten wire crucible heater. The sublimation rate was about two angstroms per second and was monitored with a KRONOS model QM 311 quartz crystal oscillator which was calibrated with a Varian model 980-4020 A-scope multiple interferometer. The temperature of the merocyanine powder was maintained at about 220°C and was monitored with a chromel-alumel thermocouple. The temperature of the substrate could be maintained at room

temperature or down to liquid nitrogen temperatures. Most cells were made on a LN_2 cooled substrate. A 200Å gold film with approximately 50% transparency in the dye absorption region was evaporated on top of the merocyanine film from a molybdenum boat. A 2000 Angsrom-thick contact ring of gold was subsequently deposited with a circular mask leaving a 3 mm diameter area as the effective area for light absorption experiments. The gold could be deposited on top of the merocyanine without breaking the vacuum, but in most cases, the merocyanine was exposed to air for about five minutes before the gold was deposited. A quartz dummy cell could be positioned next to the TiO_2 substrate in order to record the absorption spectrum of the merocyanine film. Ohmic contact to the back side of the TiO_2 crystal was provided by vacuum evaporated indium electrodes.

The transmission and absorption spectra were measured with a Cary 118 spectrophotometer. A 450 W Xenon lamp in conjunction with a Bausch and Lomb high intensity monochromator was used for the photoconductivity measurements. The dark current and the photo-current were measured with a PAR 181 current sensitive preamplifier, the photovoltage was measured with a Keithley 220 electrometer, and the voltage scans were provided by a PAR 175 Universal programmer. The light intensity was measured with a HewlettPackard 8330A radiant flux meter. For the capacitance-voltage characteristics, a General Radio 1650-A impedance bridge was used. It had a 1 kHz internal oscillator and could be coupled to an external function generator if a different frequency was desired. All measurements were done with the cell mounted in a Faraday cage. The temperature of the cell could be varied by housing the cell in a styrofoam enclosure with a quartz window and an inlet for cooled nitrogen gas. The temperature of the cell could thus be varied between +25°C and -100°C.

III. Results

A. Dark J-V

Fig. 3 shows the dark current-voltage characteristics of a cell with a 2000 angstrom thick dye layer. The cell showed some rectifying behavior with forward bias corresponding to a negative voltage applied to the TiO_2. At 0.4 volts the rectification ratio was about 6. The arrows on the graph correspond to the direction of the voltage scan.

Fig. 4 shows a semi-logarithmic plot of the forward current versus applied voltage revealing that the forward current increases exponentially with voltage at low voltages. Fig. 5 indicates that at higher voltages the current shows a power dependence on the voltage, i.e. $J \alpha V^m$. Between 0.5 V and 1.3 V, $m \simeq 6$ and above 1.3 V, $m = 2$. The square-law dependence at higher voltages was observed for films of different thicknesses, but the exponent of the middle range varied from 5.6 to 7.5 with the lower range associated with thinner merocyanine films (< 1000Å) and the upper range with thicker films, up to 3000 Å.

The exponential dependence at lower voltages may be attributed to a junction formed between the n-type substrate and the merocyanine which has been shown to exhibit p-type conductivity (21). The power dependence at higher voltages suggests that the current is space-charge limited in the presence of deep traps (22,23). According to Mark and Helfrich (23), the transition voltage to V^2 behavior is independent of the mobility of the charge carriers and the absolute value of the current and is given by

$$V_t = \frac{qd^2}{\varepsilon\varepsilon_o}\left\{\frac{9}{8}\frac{H^\ell}{N_o}\left(\frac{\ell+1}{\ell}\right)^\ell\left(\frac{\ell+1}{2\ell+1}\right)^{\ell+1}\right\}^{1/(\ell-1)}$$

for a solid with a trap distribution decreasing exponentially with increas-

ing trap depth. Here q is the elementary charge, d the thickness of the film, ε the merocyanine dielectric constant, ε_0 the permitivity of vacuum, H the total trap density, N_0 the effective density of states in the conduction or valence band, and $\ell \equiv Tc/T$ where T_C is a characteristic temperature used to approximate the rate at which the trap density changes with energy. The model also assumes that the density of traps is considerably larger than the density of free carriers. If the converse is true, we can, of course, neglect the traps.

The dielectric constant for thin dye films typically lies in the range 3-4 (24,25) N_0 of the order of 10^{21} cm^{-3} is estimated for Cu-phthalocyanine (25) and tetracene (1) films. With the value of $\ell = 5$ ($m = 6$) and $V_t = 1.3$ V from our data and $d \simeq 2000$ Å and assuming $\varepsilon = 3.5$, we obtain $H \simeq 10^{17}$ cm^{-3}. Such a value is consistent with literature values which range from $10^{15} cm^{-3}$ for single crystal tetracene (24) and anthracene (26) to $10^{19} cm^{-3}$ for films of phthalocyanine deposited on room temperature substrates (25, 9a).

The trap density was found to increase with decreasing thickness of the merocyanine film. This dependence on thickness indicates that a large fraction of the trapping states are associated with the interfaces. The trap density determined by the space-charge limited current is the density of electron traps, since in the forward mode TiO_2 is an electron injecting contact.

B. Reverse Breakdown

The large increase in conductance with applied voltage in the reverse direction beyond the 'breakdown' voltage of about 0.7 V (Fig. 3) is similar to that of a Zener diode for semiconductor devices (27). In semiconductor diodes, two distinct breakdown mechanisms are known to occur, avalanche

breakdown and tunneling, or Zener breakdown. The Zener tunneling in semiconductors is a band-to-band tunneling under reverse bias. Tunneling can also be observed in metal-insulator-semiconductor structures under reverse bias involving surface states at the semiconductor-insulator interface (27,28).

A more common mechanism in semiconductor junction breakdown is avalanche multiplication or impact ionization (27, 29). The two processes may be operationally separated, since the temperature coefficients of the breakdown voltages are of opposite sign in the two cases. For avalanche multiplication, the breakdown voltages increase at higher temperatures. The breakdown voltages for tunneling, on the other hand, have a negative temperature coefficient, i.e. the voltage decreases with increasing temperature.

In Fig. 6 we show the current-voltage curves taken at three different temperatures for a film of 2000 Å. The decrease of the breakdown voltage at higher temperatures suggests a tunneling mechanism, perhaps involving band gap states at the merocyanine-TiO_2 interface. The curves can be retraced many times reproducibly. The current surge is therefore not a destructive breakdown. This phenomenon has also been observed in bilayer lipid membranes with electrolytic contacts (30).

C. Capacitance-Voltage Characteristics

Associated with a depletion layer in a p-n junction or a Schottky barrier, there is a capacitance varying with the voltage applied across the junction. Applying a reverse bias across the junction increases the width of the junction and therefore decreases the capacitance associated with the depletion region. The dependence of the capacitace on applied voltage is obtained by solving Poisson's equation and takes the following form (27):

$$\left(\frac{A}{C}\right)^2 = \frac{2}{q\varepsilon\varepsilon_o N}(V_B - V)$$

where C is the capacitance, A the surface area, V_B the built-in voltage and q, ε, ε_o are defined above. If we are dealing with a heterojunction formed between two semiconductors having diffferent energy band gaps, we obtain (27):

$$\left(\frac{A}{C}\right)^2 = \frac{2(\varepsilon_1 N_{D1} + \varepsilon_2 N_{A2})}{q N_{D1} N_{A2} \varepsilon_1 \varepsilon_2 \varepsilon_o}(V_B - V)$$

where N_{D1} is the donor density in semiconductor 1 and N_{A2} is the acceptor density in semiconductor 2. If one plots the experimentally obtained values of $1/C^2$ versus reverse bias, we would expect a straight line where the slope and the intercept on the abscissa determine the dopant density and the barrier height respectively. Fig. 7 shows the variation of capacitace with reverse bias measured with an impedance bridge coupled to an external oscillator at 200 Hz. The capacitance is independent of applied voltage up to and beyond 0.8V. This means that the junction region is completely depleted of mobile charge carriers and the cell behaves as a simple capacitor with the dye as a dielectric. Measurements with 1 kHz oscillator frequency produce similar results.

This result favors a model where all of the built-in voltage falls across the dye film and there is a virtual absence of band bending in the TiO_2 crystal as well (Fig. 8). However, capacitance measurements at low frequencies, down to 0.1 Hz, on tetracene, Mg-phthalocyanine, and mero-

cyanine indicate that there might be some band bending in the merocyanine due to a higher density of trapped charges near the interface (11, 31). These charges would not be able to follow the ac field of 200 Hz. Our dark J-V characteristics seem to support the model with a higher trap density near the interface, but our bridge method did not allow us to measure the capacitance at sufficiently low frequencies.

D. Photoeffects

1. Transient Response

The photocurrent and the photo-voltage of the Au-merocyanine-TiO_2 cells exhibit a rather slow rise and decay time of the order of seconds (Fig. 9). The rise time of Au-TiO_2 Schottky barrier cells on the same scale is only limited by the response of the recorder. Although rise times of 10^{-5}-10^{-6} sec. have been observed with suitable experimental arrangements with metal-free and copper pthalocyanines (5,6), long transient times are known to occur for photoconductors with large densities of traps (21,32).

As the circuit was connected in the dark, we observed a dark current discharge. Since the cells were prepared in room light, the discharge is most likely due to the release of trapped photo-excited charges. When light is turned on, most cells reached a steady state level in a few seconds and could generate a photo-current for more than an hour with no appreciable decline. Some cells showed a slightly more complicated behavior in that they exhibited a slow decrease in the photocurrent of approximately 20% over about an hour after reaching a peak in a few seconds. The new level was stable within a few percent for several hours. All cells exhibited long-term decay. After being stored under ambient atmospheric conditions for 2-3 days, the photocurrent was usually lowered to 60-70% of its initial steady state value. The exact value varied from cell to cell and was dependent on the

cell history.

At higher light intensities (greater than 10 mW/cm^2) the initial decay is faster but the long term history of the cell did not appear to be affected. The long term deterioration therefore appears to be connected to oxygen effects rather than photocurrents. All our reported measurements are taken with low monochromatic intensities ($\sim$0.1 $mW\text{-}cm^{-2}$ or $\sim 10^{14}$ photons-cm^{-2} -sec^{-1}) and only steady state values are reported. The excitation wavelength 520 nm was close to the peak of the merocyanine absorption. The TiO_2 crystal, with a band gap of 3.0 eV was itself transparent in this region.

2. Kinetics of Photoconductivity

Upon bringing the photo-current to a steady state level, there is a rapid initial rise followed by a slow rise of the order of seconds (Fig. 9). When the light is turned off and the decay in the dark is analyzed, it is found that the initial rate of decay is high but that it decreases rapidly during the first few tenths of a second, becoming a constant for the remainder of the process. The decay is slower at a lower temperature (Fig. 10). The initial fast decay is of the first order (Fig. 11), i.e.

$$dn/dt \sim \alpha n \qquad 2.1$$

where n is the density of carriers and α is the rate constant. Assuming the photocurrent to be proportional to the density of carriers, we get

$$J \sim e^{-\alpha t} \qquad 2.2$$

For the slow decay process, the current obeys the relation

$$J \sim t^{-1} \qquad 2.3$$

This is the decay one would expect for a process involving the recombination of oppositely charged carriers. In this case, we may write

$$dn/dt = -kn^2 \qquad 2.4$$

where n is the concentration of positively and negatively charged carriers, and k is the rate constant (in units of cm^3-sec^{-1}-$carrier^{-1}$). Upon integration, we obtain

$$1/n = Kt + \text{constant}$$

and for large t the constant can be ignored. Since the photo-current is proportional to the concentration of carriers, we arrive at equation 2.3.

The rate constant, as measured by the slope of the 1/J versus t curve is essentially independent of the magnitude of the initial photocurrent for a reduction of about a factor of two. It increases slightly for initial photocurrents reduced by an order of magnitude or more.

3. Temperature dependence of photoconductivity

The steady state photocurrent rises with increasing temperature. The growth is given by the equation

$$J_{photo} \sim \exp(-\Delta E_{ph}/kT)$$

Plotting the logarithm of the steady state current as a function of the reciprocal temperature gives a straight line. Its slope yields the thermal activation energy of photoconductance ΔE_{ph}. The activation energy is found to be 0.11 eV and is the same for films of various thickness. As shown in Fig. 10, the decay constant of the photocurrent in the dark has a temperature dependence and increases with increasing temperature. If the logarithm of the decay constant, as measured by the slope of the decay curves for the slow decay, is plotted versus 1/T the resulting straight line gives an activation energy of 0.10 eV, close to the value for the activation energy of the steady state photocurrent.

IV. Discussion

Based on our data and using values for work functions and electron affinities in the literature, we can make a model of the Au-merocyanine-TiO_2 cell as shown in Fig. 8. The work function of Au is taken as 4.85 eV (33), the electron affinity of TiO_2 as 4.33 eV (34), the ionization energy and the electron affinity of the merocyanine film are taken as 5.6-5.8 eV and 3.3-3.5 eV respectively (21), corresponding to a "band gap" of about 2.3 eV roughly equal to the energy of the maximum of the absorption band in the visible.

Undoped dyes are known to be insulators with resistivities of the order of 10^9 - 10^{13} ohm-cm (21). Since the TiO_2 crystals have resistivities of the order of 1 ohm-cm, we would expect that essentially the entire voltage drop due to the difference in electrochemical potentials, or Fermi levels, to fall across the merocyanine film. There would thus be a virtual absence of a

depletion layer in the TiO_2 crystal. This is supported by our capacitance-voltage data, which show that the cell acts as a simple capacitor with the merocyanine as a dielectric.

Other workers, however, have found a certain band bending in undoped organic films due to higher density of trapped charges near the interfaces by performing capacitace-voltage measurements at frequencies low enough for the slow trapped charges to follow (11, 31).

Although our dark J-V measurements indicate the presence of a larger density of electron traps near the interfaces, we cannot point conclusively to any evidence of "band bending" in the merocyanine phase.

The temperature and transient response characteristics of a photoconductor are intimately related to the capture and release of carriers by defects. In general, a photoconductor will have electron and hole states distributed in energy in the band gap (22). Deep centers near the middle of the band gap become recombination centers where a captured electron will recombine with a free hole before it can be thermally re-excited to the conduction band, and similarly for holes. The trapping states are characterized by the fact that a free electron or hole captured into an unoccupied trap will be thermally re-excited into the conduction or valence band respectively before capturing a free charge of the opposite sign. The electron or hole trapping states are in thermal contact with the conduction or valence band, respectively, i.e. their occupancy is determined by the Boltzmann factor

$$\exp[-(E_c - E_t)/kT] \text{ for electrons}$$

$$\text{and } \exp[-(E_t - E_v)/kT] \text{ for holes} \qquad 4.1$$

where E_c represents the bottom of the conduction band, E_v the top of the valence band, and E_t the trapping level.

The dark J-V experiments revealed the existence of an exponential distribution of electron trapping states below the conduction band. With forward bias, only electrons were injected into the dye from the TiO_2. No holes would be injected from the Au electrode since Au forms a blocking contact with TiO_2. The response of the photoconductor was thus dominated by electrons.

If both electrons and holes are generated, the response of a photoconductor will be dominated by the majority carriers, the carriers with the highest mobility time. Since the merocyanine dyes are known to exhibit p-type conductivity (21), it is reasonable to suggest that we can ignore the effect of the electron traps in determining the effect of traps on photoconductivity. Using the relationships in 4.1, we can then write for the relationship between the density of trapped (P_t) and free (P) holes,

$$P_t/N_t = (P/N_v) \exp[(E_t - E_v)/kT] \qquad 4.2$$

where N_t is the density of trapping states and N_v approximately the number of states in the top kT slice of the valence band. We can write this as

$$P = P_t \frac{N_v}{N_t} \exp(-\Delta E_t/kT)$$

where $\Delta E_t = E_t - E_v$.

The photocurrent is proportional to the density of free holes in the valence band. The photocurrent can thus be written as $J_{Pn} = A(T)\exp(-\Delta E_t/kT)$ where $A(T)$ is a slowly varying function of temperature. Plotting the logarithm of J_{Ph} versus $1/T$ will therefore give the depth of the dominant traps as an activation energy.

The response time of the photoconductor will increase because of the filling of the traps. Following the argument of Rose (22), suppose we wish to double the number of holes by increasing the light intensity. From Equation 4.2 we see that we must also double the number of trapped holes. Hence, an additional time, $(P_t/P)\tau_{P0}$, where τ_{P0} is the response time in the absence of traps, is required to excite enough holes to double the number of trapped holes, and the total response time is therefore

$$\tau_p = (1 + P_t/P)\tau_{P0}$$

Since $P_t >> P$ for the traps to be dominant, the response time, as measured by the decay constant, will have the same temperature dependence as the steady state photocurrent.

As shown in Fig. 10, the photocurrent decays according to a second order reaction at long times. This indicates that a bimolecular recombination determines the decay process after the initial fast decay. The more rapid initial decay is a first order process, as shown in Fig. 11. This separation can be qualitatively understood as follows: The carrier recombination takes place via recombination centers rather than direct electron-hole recombination (22,35). Trapping centers near the middle of the band gap are the most efficient channels for recombination. Again, we are concerned only with the trapping and recombination of holes, since they are

the majority carriers and dominate the photoconductivity. Consider the recombination scheme in Fig. 12 where we have two separate channels dominating the electron-hole recombination (32). Channel 1 has a smaller hole trapping cross section than Channel 2 and a larger electron trapping cross section. If there is a high concentration of N_{r2} centers, they can dominate the recombination initially. Holes in the valence band and trapping centers N_t recombine with electrons in the N_{r2} recombination centers. As the N_{r2} centers become depleted of electrons, the N_{r1} channel becomes dominant and the recombination changes from first order to second order, since the electron capture cross section of channel 1 is assumed to be high.

We have been working with the assumption that band theory is at least approximately applicable to organic semiconductors. Although energy "bands" may not exist in the strict sense, numerous results in the literature attest to the usefulness of an analysis based on narrow conduction and valence bands for describing photoelectric devices based on organic solids (1-11). Our analysis of the Au-merocyanine-TiO_2 cells is not dependent on there being actual energy bands present. For an analysis of the data we have presented, the bands can be thought of as a way to represent the internal electric field in the merocyanine phase.

The band widths of organic solids, where the overlap integrals are determined by Van der Waals interaction, are so small (of the order of kT) that where the specimens are polycrystalline or amorphous, the overall transport process will be that appropriate to a localized carrier treatment. The hopping model of conductivity considers carrier motion proceeding directly from one localized state to another based on the quantum mechanical transition between localized sites (36). In molecular solids, the excitation tends to remain localized. Therefore, the generation of free carriers

involves both external electric fields and internal attractive coulomb fields.

The necessity for considering hopping as a mechanism for charge carrier motion arises from considerations of the mean free path in organic solids. A carrier of effective mass m* and mobility μ has a mean free path L given, at ordinary temperatures, by the approximate relation (37)

$$L \simeq 10^{-8} \mu (m^*/m_o)^{1/2} \text{ in cm,}$$

where m_o is the free electron mass and the units of mobility are $cm^2\text{-Volt}^{-1}\text{-sec}^{-1}$. In most molecular solids values of μ are generally less than 5 $cm^2\text{-Volt}^{-1}\text{-sec}^{-1}$, so that the mean free path, calculated from mobility data, is then of the order of 0.1 to 1 Å. This is appreciably less than the lattice spacing in a molecular crystal. It then becomes questionable whether the band theory notion of a mean velocity of the carriers can be applied.

The idea that band theory may be applied to organic materials in the form of pure single crystals is, however, supported by data presently available (38), although its applicability to poly-crystalline and amorphous molcular crystals remains questionable.

Acknowledgements

The support of this research by the Division of Chemical Sciences, Office of Basic Energy Sciences of the United States Department of Energy under Contract W-7405-ENG-48 is gratefully acknowledged.

References

1. A. K. Ghosh and T. Feng, J. Appl. Phys. 44, 2781 (1973).

2. C. W. Tang and A. C. Albrecht, (a) Mol. Cryst. Liq. Cryst. 25, 53 (1974); (b) J. Chem. Phys. 62, 2139 (1975); (c) J. Chem. Phys. 63, 953 (1975); (d) Nature 254, 507 (1975).

3. L. E. Lyons and O. M.G. Newman, Aust. J. Chem. 24, 13 (1971).

4. A. K. Ghosh, D. L. Morel, T. Feng, R. S. Shaw, and C. A. Rowe, J. Appl. Phys. 45, 239 (1974).

5. M. I. Fedorov and V. A. Benderskii, (a) Sov. Phys. Semicond. 2, 580 (1968); (b) Sov. Phys. Semicond. 4, 1198 (1971); (c) Sov. Phys. Semicond. 4, 1720 (1971).

6. V. Y.Merritt and H. J. Hovel, Appl. Phys. Lett. 29, 414 (1976).

7. V. Y.Merritt, IBM J. Res. Develop. 22, 353 (1978).

8. F. J. Kampas and M. Gouterman, J. Phys. Chem. 81, 690 (1977).

9. F. R. Fan and L. R. Faulkner, (a) J. Chem. Phys. 69, 3334 (1978). (b) J. Chem. Phys. 69, 3341 (1978).

10. D. L. Morel, A. K. Ghosh, T. Feng, E. L. Stogryn, P. E. Purwin, and C. Fishman, Appl. Phys. Lett. 32, 495 (1978).

11. A. K. Ghosh and T. Feng, J. Appl. Phys. 49, 5982 (1978).

12. D. R. Kearns and M. Calvin, J. Chem. Phys. 29, 950 (1958).

13. C. Mees and T. James, eds., "The Theory of the Photographic Process," (New York: Macmillan, 1966).

14. R. C. Nelson, J. Phys. Chem. 71, 2517 (1967).

15. R. C. Nelson, J. Opt. Soc. Am. 51, 1182 (1961).

16. E. Inoue, H. Kokado, and U. Yamaguchi, J. Phys. Chem. 67, 767 (1965).

17. H. Meier, "Spectral Sensitization" (London: The Focal Press, Ltd. 1968).

18. H. Tributsch and H. Gerischer, Ber. Bunsenges. Phys. Chem. 73, 850 (1969).

19. H. Gerishcer, Surface Sci. 13, 265 (1969).

20. D.Cronemeyer, Phys. Rev. 113, 1222 (1959).

21. H. Meier, "Organic Semiconductors," (Weinheim: Verlag Cehmie, 1974).

22. A. Rose, "Concepts in Photoconductivity and Allied Problems," (New York: Interscience, 1963).

23. P. Mark and W. Helfrich, J. Appl. Phys. 33, 205 (1962).

24. H. Baessler, G. Hermann, N. Riehl, and G. Vaubel, J. Phys. Chem. Solids, 30, 1579 (1969).

25. A. Sussman, J. Appl. Phys. 38, 2738 (1967).

26. J. M. Thomas, J. O. Williams, and L. M. Turyon, Trans. Faraday Soc. 64, 2505 (1968).

27. S. M. Sze, "Physics of Semiconductor Devices," (New York: Wiley, 1969).

28. W. E. Dahlke and S. M. Sze, Solid State Electronics 10, 865 (1967).

29. H. K. Henisch, "Electroluminescence," (New York: Macmillan, 1962).

30. B. Rosenberg, Disc. Faraday Soc. 51, 190 (1971).

31. A. J. Twarowski and A. C. Albrecht, J. Chem. Phys. 70, 2255 (1979).

32. G. N. Meshkova, Sov. Phys. Semicond. 2, 1244 (1969).

33. "CRC Handbook of Chemistry and Physics," 52nd ed. (1971).

34. M. A. Butler and D. S. Ginley, J. Electrochem. Soc. 125, 228 (1978).

35 R. H. Bube, "Physical Chemistry: An Advanced Treatise," Vol. 10, H. Eyring, D. Henderson, and W. Jost, eds. (New York: Academic Press, 1970), p. 515.

36. H. Scher, "Photoconductivity and Related Phenomena," J. Mort and D. M. Pai, eds. (New York: Elsevier Scientific, 1976), p. 72.

37. F. Gutman and L. E. Lyons, "Organic Semiconductors," (New York: John Wiley & Sons, 1967).

38. H. Inokuchi and Y. Maruyama, "Photoconductivity and Related Phenomena," J. Mort and D. M. Pai, eds. (New York: Elsevier Scientific, 1976).

FIGURE CAPTIONS

Figure 1. Chemical structure of the merocyanine dye used in making the photovoltaic cells.

Figure 2. Diagram of sandwich cell structure.

Figure 3. Dark current-voltage characteristics of a Au-merocyanine-TiO_2 cell with a 2000 angstrom thick merocyanine film. The arrows indicate the direction of the voltage scan. The voltage scan was 10mV per second.

Figure 4. Semi-log plot of current versus applied forward bias for a cell with 2000 angstrom thick merocyanine film.

Figure 5. Log-log plot of current versus applied forward bias for a cell with 2000 angstrom merocyanine film. V_{t-c} represents the transition to trapfree Child's law behavior.

Figure 6. Current-voltage curves recorded at three different temperatures with a cell with a 2000 angstrom merocyanine film.

Figure 7. Capacitance as a function of reverse bias for a cell with 1000 angstrom merocyanine film. The oscillator frequency was 200Hz.

Figure 8. Energy level representation of a Au-merocyanine-TiO_2 cell before (a) and after (b) contact respectively.

Figure 9. Time behavior of the dark current transient and the short circuit photocurrent under monochromatic irradiation at 520nm.

Figure 10. Long time decay of the photocurrent upon turning off the light at two different temperatures. The decay constant is defined as the slope of the curves.

Figure 11. Simi-log plot of the initial decay of the photocurrent upon turning off the light.

Figure 12. Electron-hole recombination scheme dominated by two separate channels. Sn1, Sn2, Sp1 and Sp2 are the electron and hole trapping cross sections of the two recombination centers, Nr1 and Nr2.

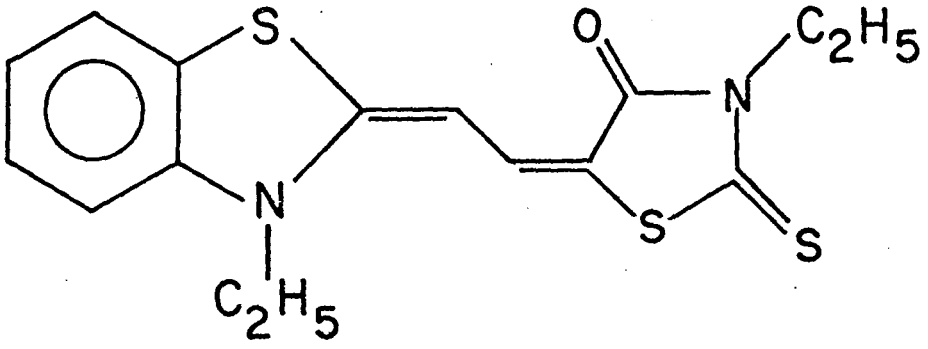

Fig. 1

XBL796-4875

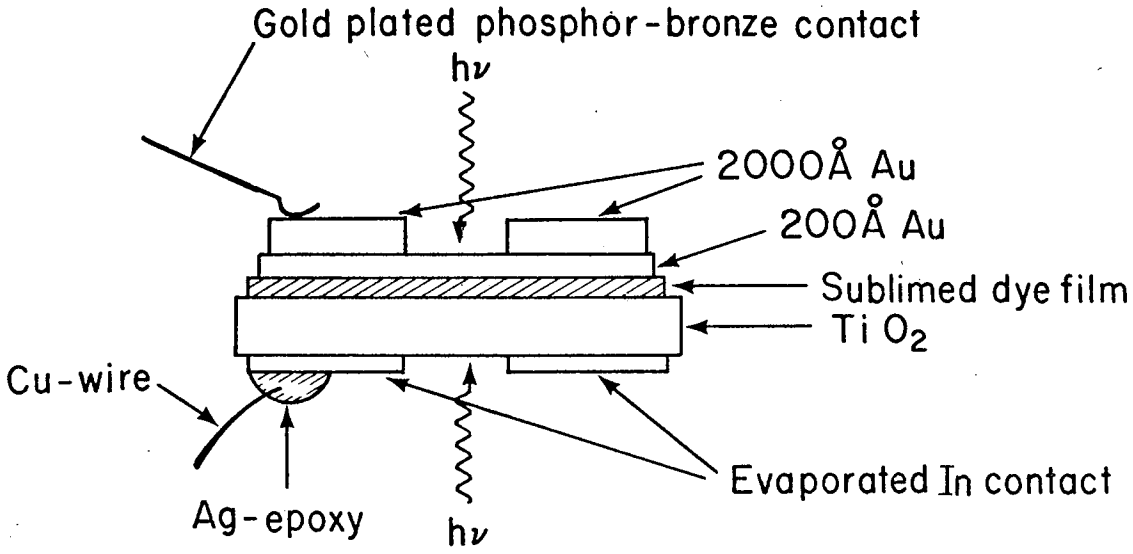

Fig. 2

XBL796-4881

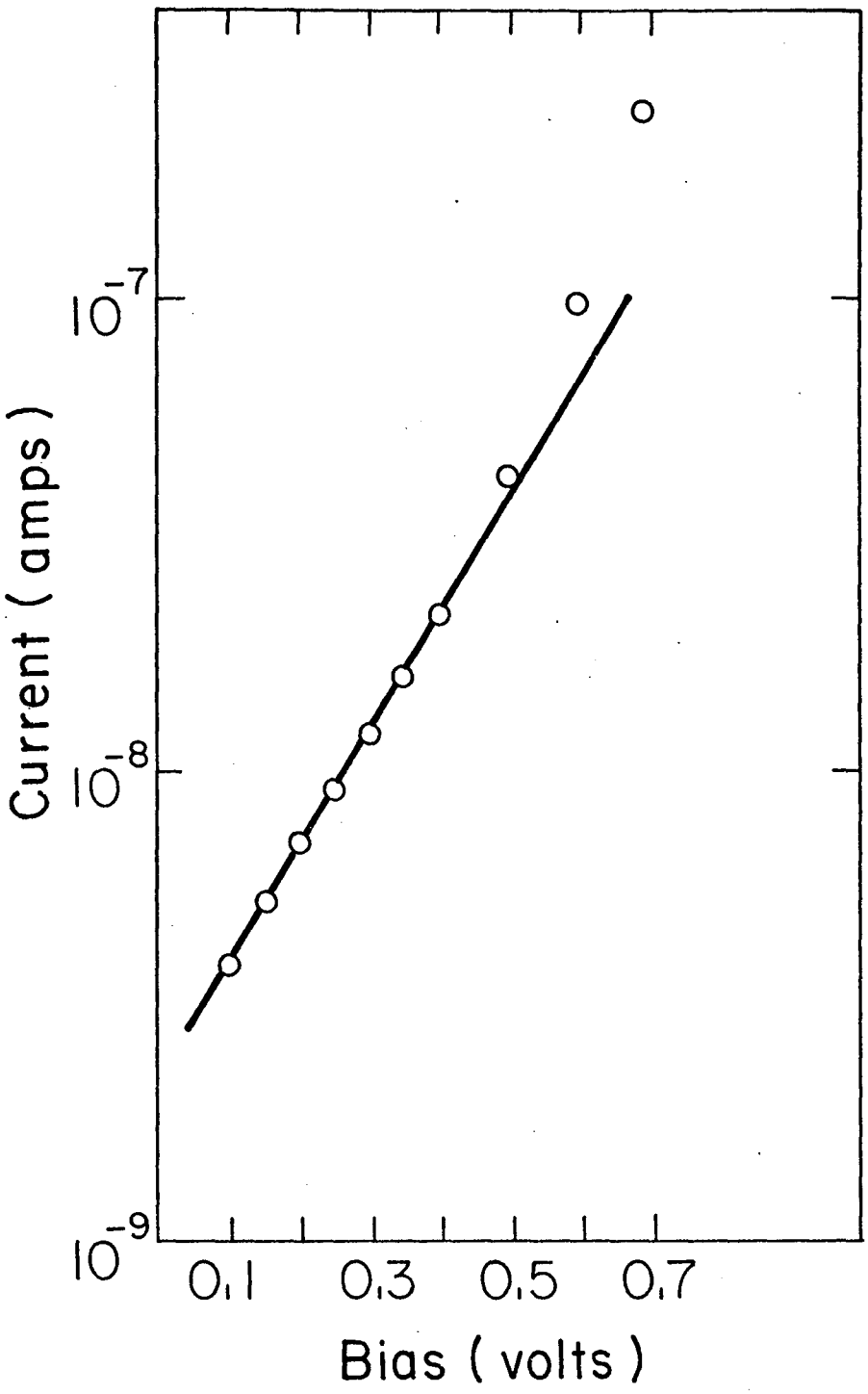

Fig. 4

XBL797-4896

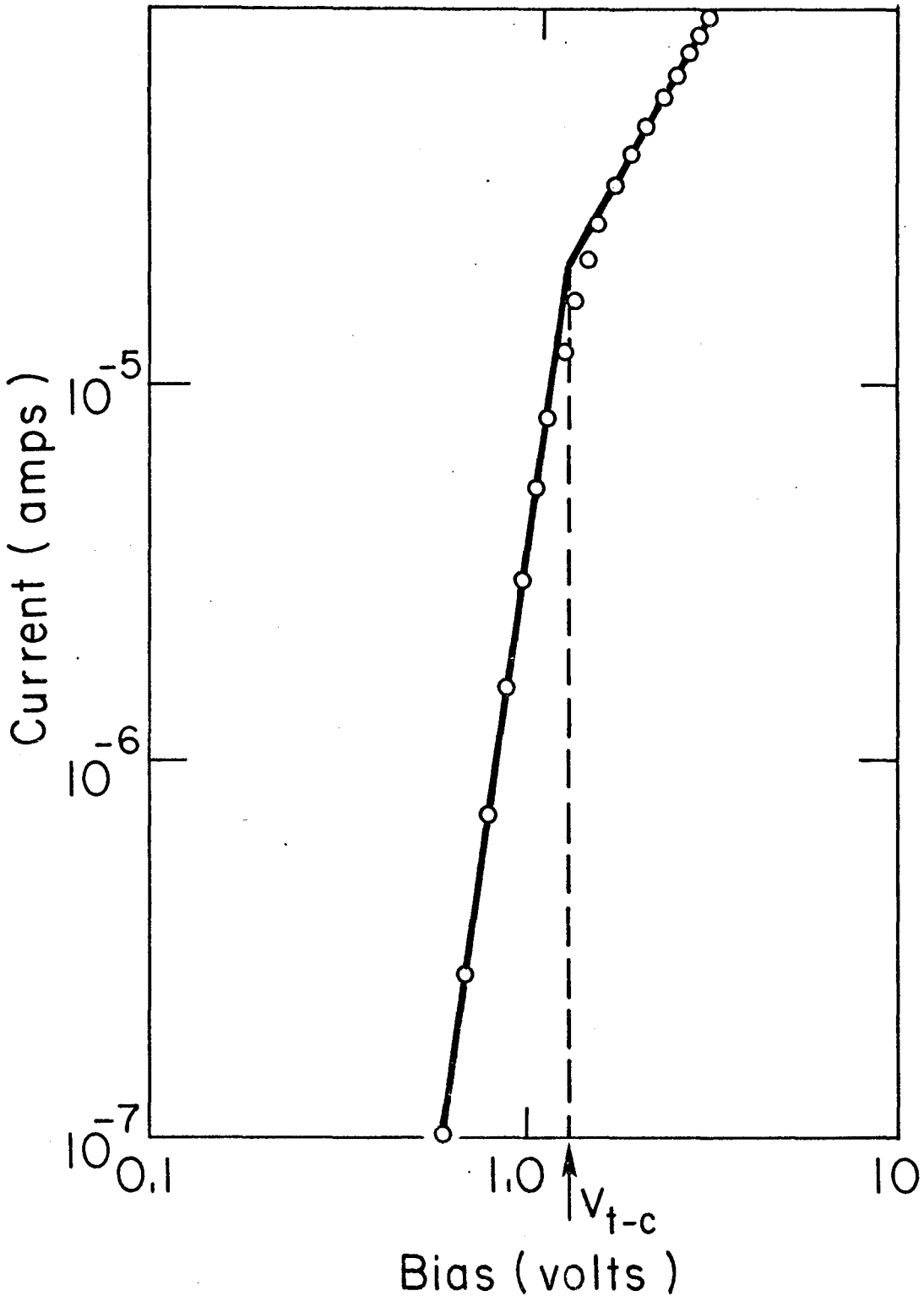

Fig. 5

XBL797-4903

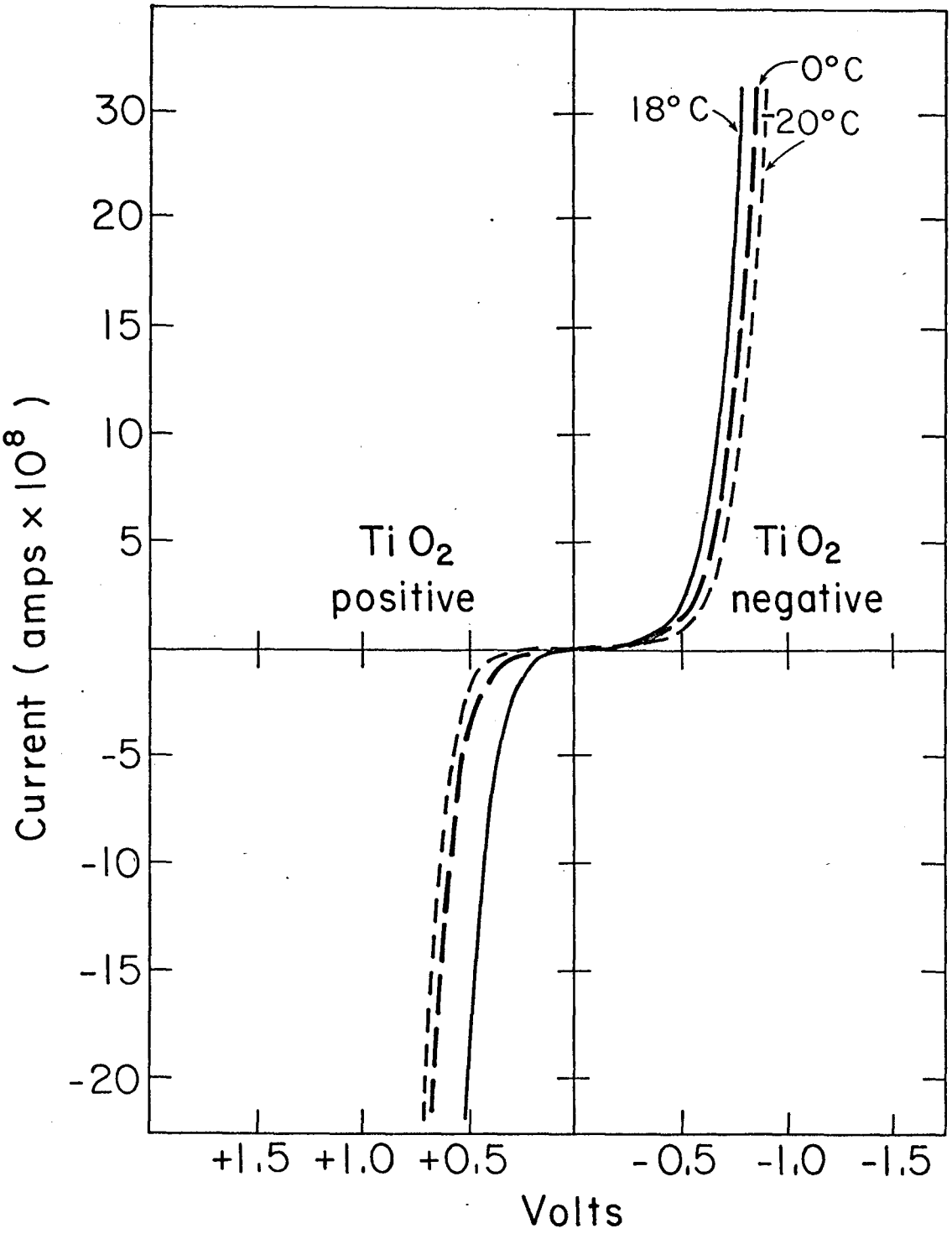

Fig. 6

XBL797-4912

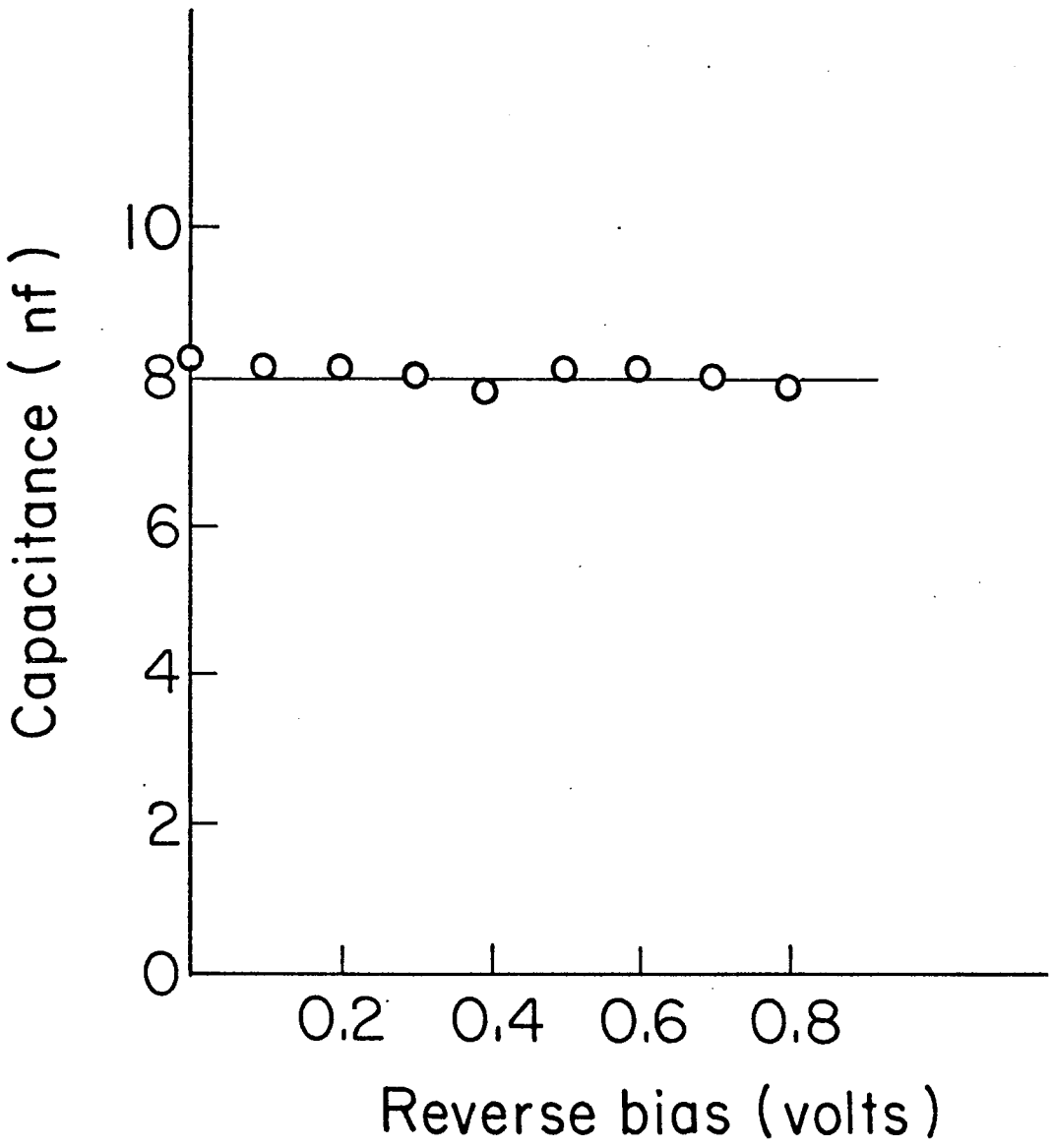

Fig. 7

XBL796-4838

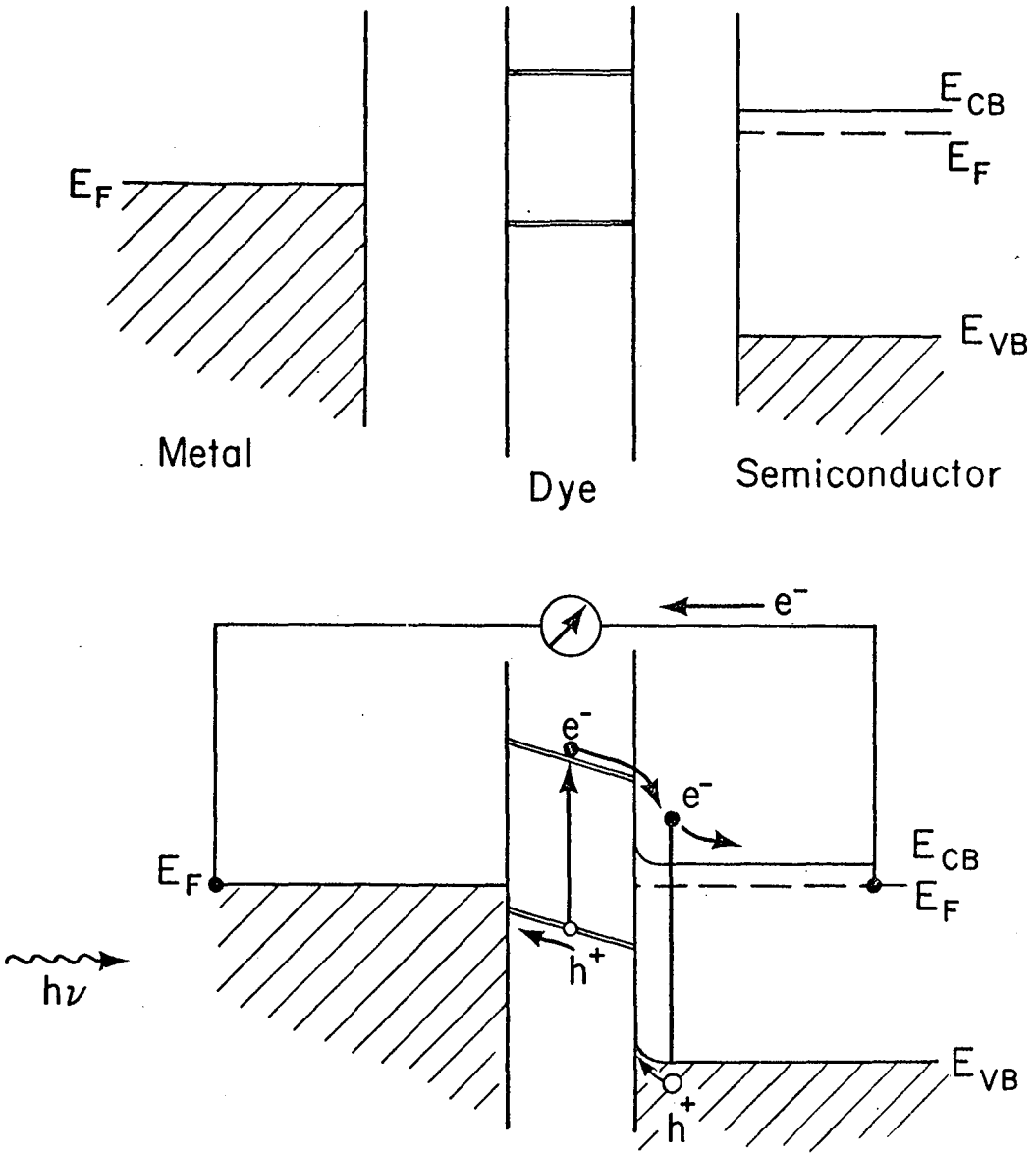

Energy levels under short circuit current condition

Fig. 8

XBL 791-4616

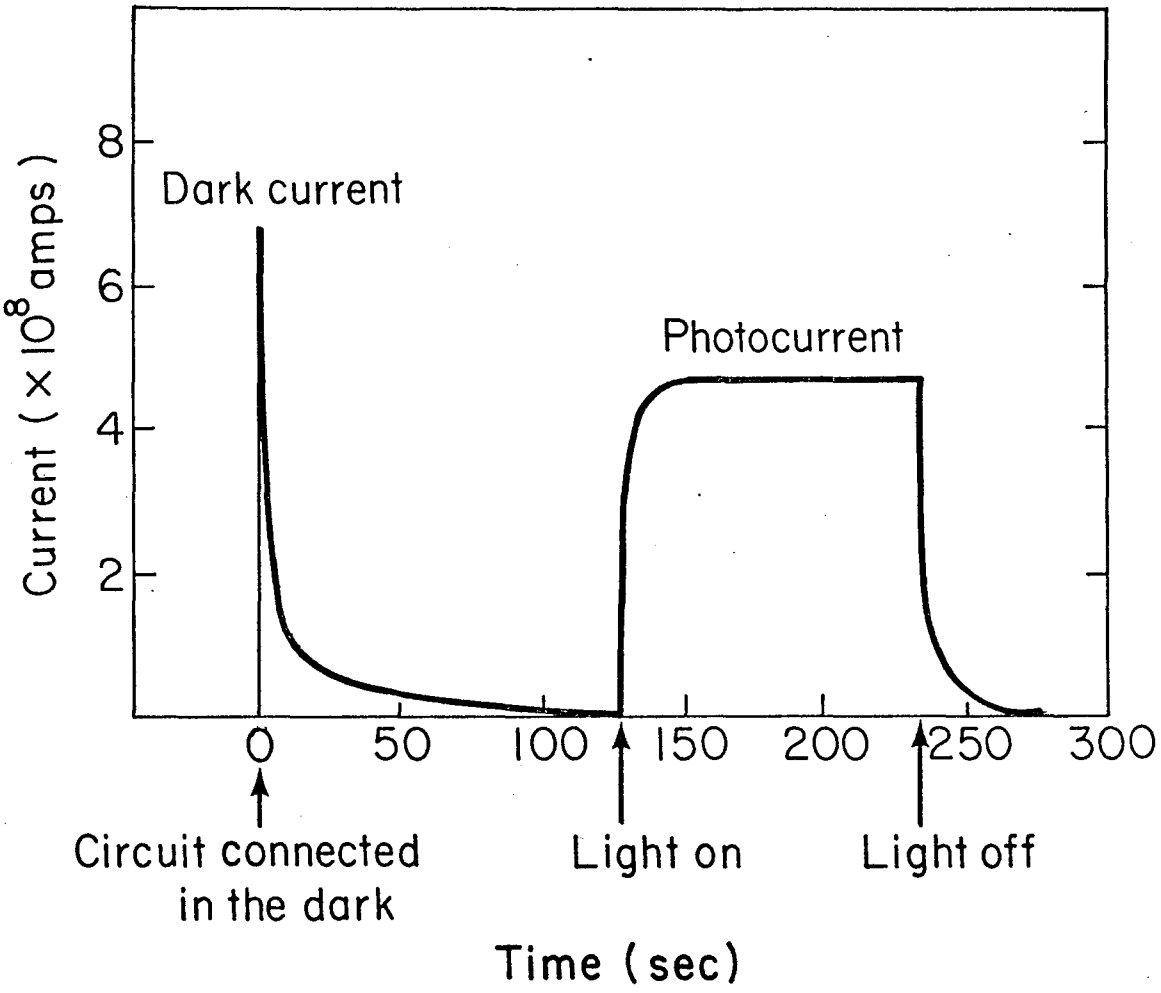

Fig. 9

XBL797-4898

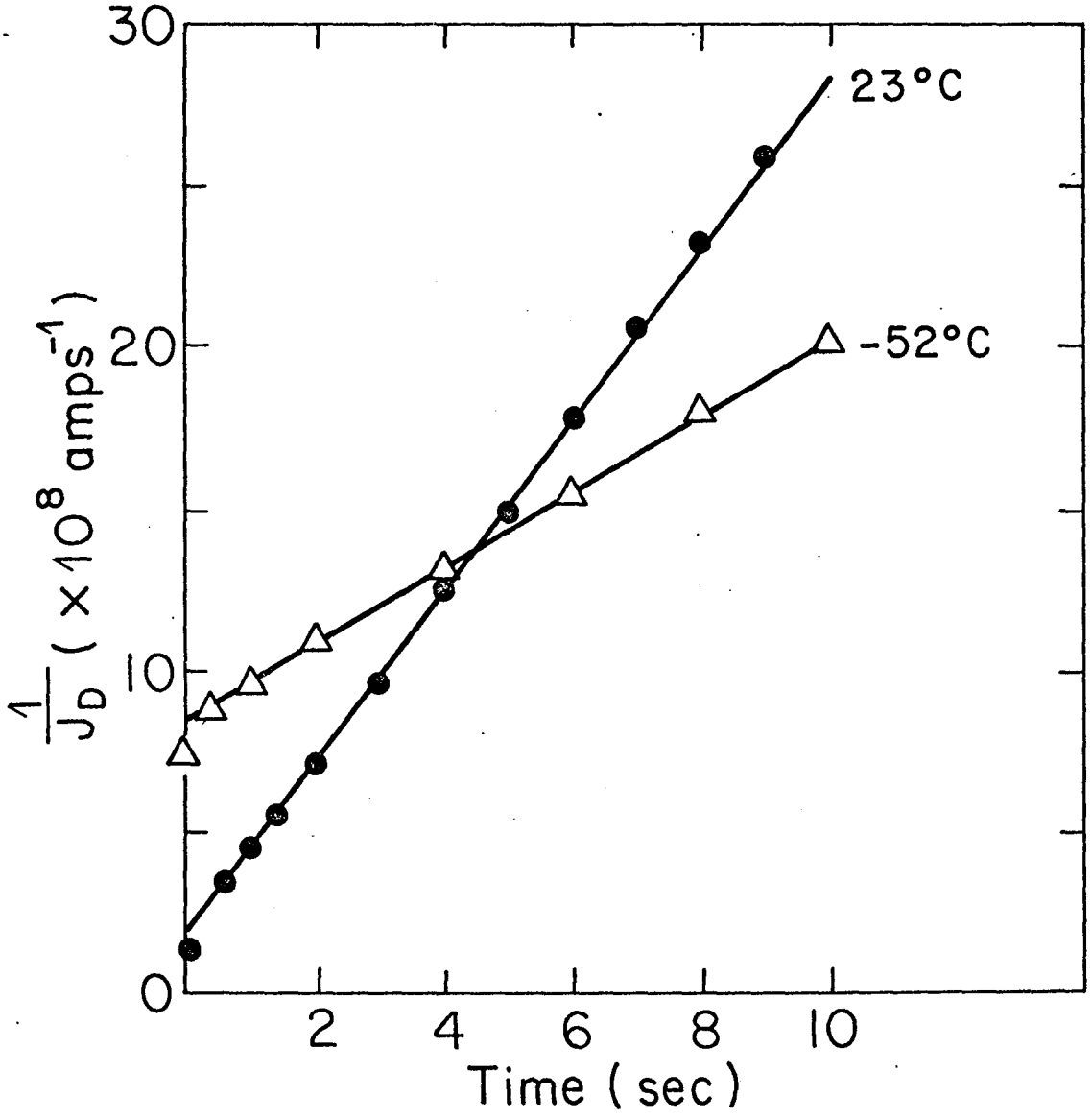

Fig. 10

XBL796-4883

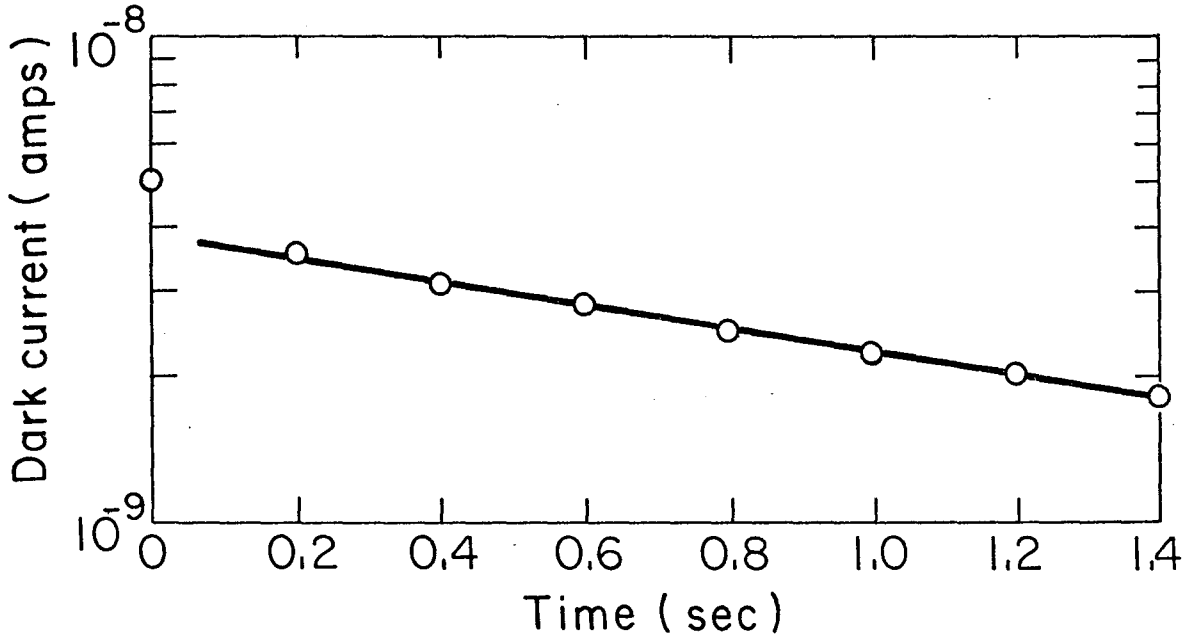

Fig. 11

XBL797-4906

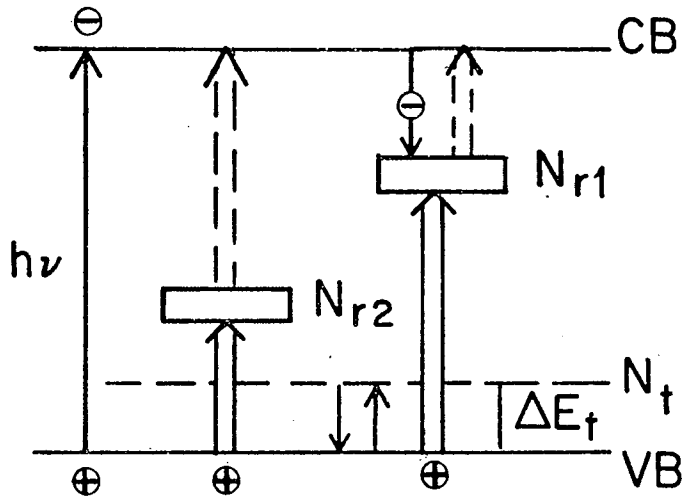

Recombination scheme

$$\begin{cases} S_{p2} > S_{n2} \text{ and } S_{p1} \simeq S_{n1} \\ S_{n2} < S_{n1} \\ S_{p2} > S_{p1} \end{cases}$$

Channel N_{r1}: $p_{r1} + \ominus \longrightarrow n_{r1}$ fast

$n_{r1} + \oplus \longrightarrow p_{r1}$ slow

Channel N_{r2}: $n_{r2} + \oplus \longrightarrow p_{r2}$ fast

$p_{r2} + \ominus \longrightarrow n_{r2}$ slow

Fig. 12

XBL797-4889

This report was done with support from the United States Energy Research and Development Administration. Any conclusions or opinions expressed in this report represent solely those of the author(s) and not necessarily those of The Regents of the University of California, the Lawrence Berkeley Laboratory or the United States Energy Research and Development Administration.